PROCEEDINGS OF SPIE

SPIEDigitalLibrary.org/conference-proceedings-of-spie

Interpretation of optical caustic patterns obtained during unsteady crack growth: an analysis based on a higher-order transient expansion

Cheng Liu, Ares J. Rosakis

Cheng Liu, Ares J. Rosakis, "Interpretation of optical caustic patterns obtained during unsteady crack growth: an analysis based on a higher-order transient expansion," Proc. SPIE 1554, Second International Conference on Photomechanics and Speckle Metrology, (1 December 1991); doi: 10.1117/12.49532

SPIE.

Event: San Diego, '91, 1991, San Diego, CA, United States

Interpretation of optical caustic patterns obtained during unsteady crack growth: An analysis based on a higher-order transient expansion

Cheng Liu and Ares J. Rosakis

California Institute of Technology, Graduate Aeronautical Laboratories
Pasadena, California 91125

ABSTRACT

The optical caustic method is re-examined considering the presence of transient effects. Based on the higher-order asymptotic expansion provided by Freund and Rosakis[1], regarding the stress field near a non-uniformly propagating crack tip, the caustic mapping and the initial curve equations are derived. The dynamic stress intensity factor, $K_I^d(t)$, is related to experimentally measurable quantities of the caustic pattern by an explicit expression. It is shown that the classical analysis of caustics is a special case of the new interpretation method. The Broberg problem is used as an example problem to check the feasibility of analysing caustics in the presence of higher-order transient terms. It is shown that the caustic patterns are sensitive to transient effects, and that use of the classical analysis of caustics in the interpretation of the optical patterns for this problem may result in large errors in the value of the stress intensity factor, especially at short times after initiation.

1. INTRODUCTION

The dynamic stress intensity factor, $K_I^d(t)$, plays a pivotal role in dynamic fracture mechanics since it forms the basis of the formulation of crack growth criterion. It is often postulated that for dynamic crack growth at a specific velocity, v, the instantaneous value of the dynamic stress intensity factor, K_I^d, should be equal to a unique, material dependent function of crack tip velocity, called the dynamic fracture toughness and denoted by $K_{IC}^d(v)$. This forms the basis of the dynamic crack growth criterion. While K_I^d is determined from the initial/boundary value problem and is a known function of velocity $v(t)$, the dynamic fracture toughness $K_{IC}^d(v)$ can only be determined by experiment for a specific solid.

In the last two decades, extensive experimental effort has gone into the verification of the above postulate and the measurement of the fracture toughness. However, experimental investigators seem to disagree on whether K_{IC}^d is a unique function of velocity for each material or whether it depends on other parameters such as crack tip acceleration[2]. For the most part, all experimental techniques that have been used to obtain information about the dynamic fracture toughness, assumed that the region from where the information was obtained, was K_I^d-dominant. The assumption of K_I^d-dominance states that the stress field at a finite region near the crack tip can be approximated accurately by the asymptotic singular solution (to within some acceptable error). Recent experimental evideneces by the bifocal caustic method[3] and by the coherent gradient sensing (CGS) method[4] have demonstrated that the assumption of K_I^d-dominance is often violated during dynamic crack growth. As a result, many of the experimental measurements obtained in the last two decades based on this assumption may be inaccurate. This could explain the source of disagreement and the debate over the validity of the dynamic fracture criterion. Freund and Rosakis[1] have suggested that under fairly severe transient conditions, a representation of the crack tip field in the form of higher-order expansion should be used to interpret the experimental observations.

In this paper, the optical caustic method is re-examined by considering the non-uniform crack growth history. The caustic mapping equation and the initial curve equation are derived based on the higher-order expansion given by Freund and Rosakis[1] for the transient crack growth which allows both the crack tip speed and dynamic stress intensity factor to be arbitary differentiable functions of time. It is shown that the coefficients of this expansion depend on time derivatives of $K_I^d(t)$ and $v(t)$. Here an explicit relation between the dynamic stress intensity factor and the caustic diameter is established. The dynamic effects such as the acceleration of the crack tip and the time derivative of the dynamic stress intensity factor are taken into account in the new interpretation method, and the classical analysis (K_I^d-dominant) of the caustic patterns is a special case of the new method. Finally, the Broberg problem is employed to check the feasibility of accurately analysing caustics in transient crack growth situation.

2. CAUSTICS GENERATED BY NON-UNIFORMLY PROPAGATING CRACKS

2.1. Caustic method

Consider a plate specimen of uniform thickness, h, in the undeformed state. Let its mid-plane occupy the (x_1, x_2) plane of an orthonormal Cartesian coordinate system. If the specimen is subjected to applied loads, light rays transmitted through its thickness or reflected from its surface, undergo optical path changes. These changes are related to stress induced gradients in refractive index and/or gradients in surface elevation. Both gradients of refractive index and surface elevation are related to gradients in the stress state. If the stress gradients satisfy certain condition, then a collimated light beam transmitted through the specimen or reflected from its surface, will form a three-dimensional envelope in space, see Fig.1. This envelope, which is called the *caustic surface*, is the locus

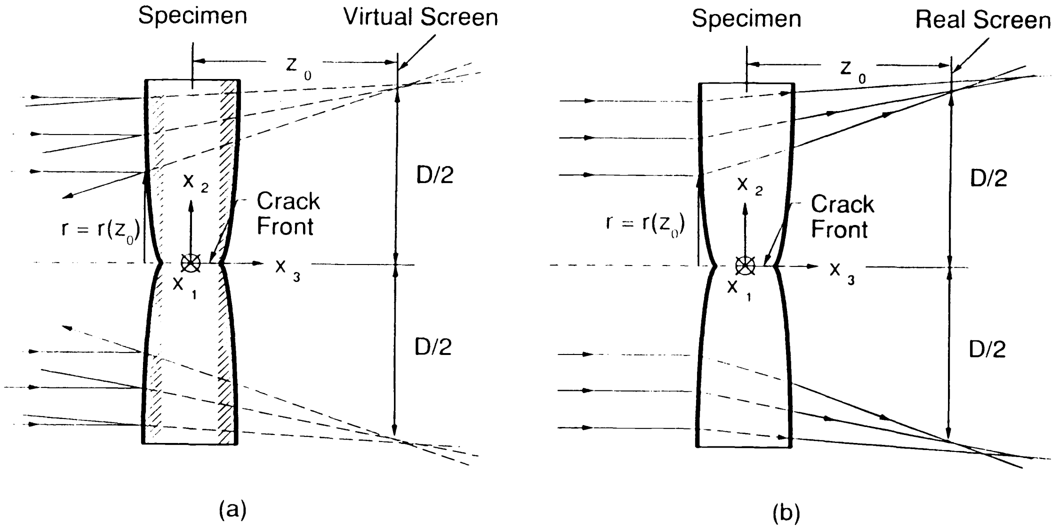

Figure 1: Caustic formation in (a) reflection, (b) transmission.

of points of maximum luminosity in the reflected or transmitted light fields. If a screen is positioned parallel to the $x_3 = 0$ plane, and so that it intersects the caustic surface, then the cross-section of the caustic surface can be observed on the screen as a bright curve (the *caustic curve*) bordering a dark region (the *shadow spot*). Suppose that the incident ray, which is reflected from or transmitted through point $p(x_1, x_2)$ on the specimen, intersects the screen at the image point $P(X_1, X_2)$. The (X_1, X_2) coordinate system is identical to the (x_1, x_2) system, except that the origin of the former has been translated by a distance z_0 to the screen (z_0 can be positive or negative). The position of the image point P is given by[5]

$$X_{,\alpha} = x_{,\alpha} + z_0 \{\Delta S(x_1, x_2)\}_{,\alpha} \ , \tag{1}$$

where $\alpha = 1, 2$, and $\Delta S(x_1, x_2)$ is the optical path change. Relation (1) describes the mapping of points on the specimen onto points on the screen.

If the screen intersects the caustic surface, then the resulting caustic curve on the screen is the optical mapping of the locus of points for which the determinant of the Jacobian matrix of the caustic mapping equation (1) must vanish on the specimen, i.e.

$$J(x_1, x_2; z_0) = det\,[X_{\alpha,\beta}] = det\,[\delta_{\alpha\beta} + z_0(\Delta S)_{,\alpha\beta}] = 0 \ . \tag{2}$$

Equation (2) is a necessary and sufficient condition for the existence of a caustic curve. The locus of points on the specimen plane$(x_1, x_2, x_3 = 0)$ for which the Jacobian vanishes is called the *initial curve* whose geometry is described by equation (2). All points on the initial curve map onto the caustic curve, and all points inside and outside this curve map outside the caustic curve. It should be noted that the equation of the initial curve depends parametrically on z_0, which is a variable of the experimental set-up.

2.2. Caustic mapping equation and initial curve equation in the presence of transient effects

For a cracked linear elastic plate of uniform thickness and finite in-plane dimensions, the optical path difference ΔS, in general will depend on the details of the three-dimentional elastostatic or elastodynamic stress state that would exist at the vicinity of the crack tip. This will be a function of the applied loading, in-plane dimentions and thickness of the specimen. In the present work, we assume that the two-dimensional asymptotic analysis may provide adequate appproximation for $\Delta S(x_1, x_2)$ and the initial curve is always kept outside the near tip three-dimensional zone. Under these conditions, the optical path difference $\Delta S(x_1, x_2)$ will be[5]

$$\Delta S(x_1, x_2) = ch[\sigma_{11}(x_1, x_2) + \sigma_{22}(x_1, x_2)] \ , \tag{3}$$

where c is the stress-optical coefficient for reflection, or transmission, and σ_{11} and σ_{22} are thickness averages of the stress components in the solid.

For a planar, mode-I crack that grows with a non-uniform speed $v(t)$, along the positive x_1 direction, where (x_1, x_2) is a coordinate system translating with the moving crack tip, the asymptotic representation of the first stress invariant is[1]

$$\begin{aligned}\frac{\sigma_{11}+\sigma_{22}}{2\rho(c_l^2-c_s^2)} &= \frac{3v^2}{4c_l^2}A_0(t)r_l^{-\frac{1}{2}}\cos\frac{\theta_l}{2} + \frac{2v^2}{c_l^2}A_1(t) \\ &+ \left\{\frac{15v^2}{4c_l^2}A_2(t)\cos\frac{\theta_l}{2} + D_l^1\{A_0(t)\}\left[\left(1-\frac{v^2}{2c_l^2}\right)\cos\frac{\theta_l}{2} + \frac{v^2}{8c_l^2}\cos\frac{3\theta_l}{2}\right]\right. \\ &\left.+ \frac{1}{2}B_l(t)\left[\left(1-\frac{v^2}{c_l^2}\right)\cos\frac{\theta_l}{2} - \left(1-\frac{5v^2}{8c_l^2}\right)\cos\frac{3\theta_l}{2} + \frac{v^2}{16c_l^2}\cos\frac{7\theta_l}{2}\right]\right\} r_l^{\frac{1}{2}} + O(r_l) \ ,\end{aligned} \tag{4}$$

where

$$\begin{aligned} A_0(t) &= \frac{4}{3\mu\sqrt{2\pi}}\frac{1+\alpha_s^2}{D(v)}K_I^d(t) \ , \\ D_l^1\{A_0(t)\} &= -\frac{3v^{\frac{3}{2}}(t)}{\alpha_l^2c_l^2}\frac{d}{dt}\left\{v^{\frac{1}{2}}(t)A_0(t)\right\} = -\frac{4v^{\frac{3}{2}}(t)}{\mu\sqrt{2\pi}\alpha_l^2c_l^2}\frac{d}{dt}\left\{v^{\frac{1}{2}}(t)\frac{1+\alpha_s^2}{D(v)}K_I^d(t)\right\} \ , \\ B_l(t) &= \frac{3v^2(t)}{2\alpha_l^4c_l^4}A_0(t)\frac{dv(t)}{dt} = \frac{2v^2(t)}{\mu\sqrt{2\pi}\alpha_l^4c_l^4}\frac{1+\alpha_s^2}{D(v)}K_I^d(t)\frac{dv(t)}{dt} \ , \\ D(v) &= 4\alpha_l\alpha_s - (1+\alpha_s^2)^2 \ , \\ r_{l,s}^2(t) &= x_1^2 + \alpha_{l,s}^2(t)x_2^2 \ , \quad \theta_{l,s}(t) = \tan^{-1}\left\{\frac{\alpha_{l,s}(t)x_2}{x_1}\right\} \ , \\ \alpha_{l,s}^2(t) &= 1 - \frac{v^2(t)}{c_{l,s}^2} \ , \end{aligned}$$

and $K_I^d(t)$ is the dynamic stress intensity factor, ρ and μ are the mass density and the shear modulus, and c_l and c_s are the longitudinal and shear stress wave velocities of the elastic material.

By substituting the above expression for the first stress invariant into the optical path difference relation (3), the mapping equation (1) becomes

$$\begin{aligned} X_1 = r_l\cos\theta_l + z_0ch\rho(c_l^2-c_s^2)&\left[\frac{3v^2}{4c_l^2}A_0(t)r_l^{-\frac{3}{2}}\cos\frac{3\theta_l}{2}\right. \\ &- \left\{\frac{15v^2}{4c_l^2}A_2(t)\cos\frac{\theta_l}{2} + D_l^1\{A_0(t)\}\left[\left(1-\frac{v^2}{4c_l^2}\right)\cos\frac{\theta_l}{2} - \frac{v^2}{8c_l^2}\cos\frac{5\theta_l}{2}\right]\right. \\ &\left.\left.-\frac{1}{2}B_l(t)\left[\left(1-\frac{v^2}{4c_l^2}\right)\cos\frac{\theta_l}{2} - \left(1-\frac{3v^2}{8c_l^2}\right)\cos\frac{5\theta_l}{2} + \frac{3v^2}{16c_l^2}\cos\frac{9\theta_l}{2}\right]\right\}r_l^{-\frac{1}{2}}\right] \ , \end{aligned} \tag{5}$$

$$X_2 = \frac{r_l \sin\theta_l}{\alpha_l} + \alpha_l z_0 ch\rho(c_l^2 - c_s^2)\left[\frac{3v^2}{4c_l^2}A_0(t)r_l^{-\frac{3}{2}}\sin\frac{3\theta_l}{2}\right.$$
$$-\left\{\frac{15v^2}{4c_l^2}A_2(t)\sin\frac{\theta_l}{2} + D_l^1\{A_0(t)\}\left[\left(1-\frac{3v^2}{4c_l^2}\right)\sin\frac{\theta_l}{2} - \frac{v^2}{8c_l^2}\sin\frac{5\theta_l}{2}\right]\right.$$
$$\left.\left.+\frac{1}{2}B_l(t)\left[3\left(1-\frac{3v^2}{4c_l^2}\right)\sin\frac{\theta_l}{2} + \left(1-\frac{7v^2}{8c_l^2}\right)\sin\frac{5\theta_l}{2} - \frac{3v^2}{16c_l^2}\sin\frac{9\theta_l}{2}\right]\right\}r_l^{-\frac{1}{2}}\right] . \tag{6}$$

The initial curve defined by equation (2) is

$$1 + \hat{C}\left\{-\frac{9v^4}{8c_l^4}A_0(t)r_l^{-\frac{5}{2}}\cos\frac{5\theta_l}{2}\right.$$
$$\left.+\left[\frac{15v^4}{8c_l^4}A_2(t)\cos\frac{3\theta_l}{2} - D_l^1\{A_0(t)\}(f_{11}^d(\theta_l) + \alpha_l^2 f_{22}^d(\theta_l)) + B_l(t)(f_{11}^b(\theta_l) - \alpha_l^2 f_{22}^b(\theta_l))\right]r_l^{-\frac{3}{2}}\right\}$$
$$+\alpha_l^2\hat{C}^2\left\{-\left(\frac{9v^2}{8c_l^2}A_0(t)\right)^2 r_l^{-5} + \frac{9v^2}{8c_l^2}A_0(t)\left[\frac{15v^2}{4c_l^2}A_2(t)\cos\theta_l - D_l^1\{A_0(t)\}g_1^d(\theta_l) + B_l(t)g_1^b(\theta_l)\right]r_l^{-4}\right.$$
$$+\left[-\left(\frac{15v^2}{8c_l^2}A_2(t)\right)^2 + \frac{15v^2}{8c_l^2}A_2(t)D_l^1\{A_0(t)\}g_2^d(\theta_l) + (D_l^1\{A_0(t)\})^2\left[f_{11}^d(\theta_l)f_{22}^d(\theta_l) - (f_{12}^d(\theta_l))^2\right]\right.$$
$$-B_l(t)\left\{\frac{15v^2}{8c_l^2}A_2(t)g_2^b(\theta_l) + D_l^1\{A_0(t)\}\left[f_{22}^d(\theta_l)f_{11}^b(\theta_l) - f_{11}^d(\theta_l)f_{22}^b(\theta_l) - 2f_{12}^d(\theta_l)f_{12}^b(\theta_l)\right]\right\}$$
$$\left.\left.-B_l^2(t)\left[f_{11}^b(\theta_l)f_{22}^b(\theta_l) + (f_{12}^b(\theta_l))^2\right]\right]r_l^{-3}\right\} = 0 , \tag{7}$$

where

$$\begin{aligned}
\hat{C} &= z_0 ch\rho(c_l^2 - c_s^2) , \\
g_1^d(\theta_l) &= (f_{11}^d(\theta_l) - f_{22}^d(\theta_l))\cos\frac{5\theta_l}{2} + 2f_{12}^d(\theta_l)\sin\frac{5\theta_l}{2} , \\
g_1^b(\theta_l) &= (f_{11}^b(\theta_l) + f_{22}^b(\theta_l))\cos\frac{5\theta_l}{2} + 2f_{12}^b(\theta_l)\sin\frac{5\theta_l}{2} , \\
g_2^d(\theta_l) &= (f_{11}^d(\theta_l) - f_{22}^d(\theta_l))\cos\frac{3\theta_l}{2} + 2f_{12}^d(\theta_l)\sin\frac{3\theta_l}{2} , \\
g_2^b(\theta_l) &= (f_{11}^b(\theta_l) + f_{22}^b(\theta_l))\cos\frac{3\theta_l}{2} + 2f_{12}^b(\theta_l)\sin\frac{3\theta_l}{2} , \\
f_{11}^d(\theta_l) &= -\frac{1}{2}\cos\frac{3\theta_l}{2} + \frac{3v^2}{16c_l^2}\cos\frac{7\theta_l}{2} , \\
f_{11}^b(\theta_l) &= -\frac{3}{4}\left(1-\frac{v^2}{3c_l^2}\right)\cos\frac{3\theta_l}{2} + \frac{3}{4}\left(1-\frac{v^2}{8c_l^2}\right)\cos\frac{7\theta_l}{2} - \frac{15v^2}{64c_l^2}\cos\frac{11\theta_l}{2} , \\
f_{22}^d(\theta_l) &= \frac{1}{2}\left(1-\frac{v^2}{c_l^2}\right)\cos\frac{3\theta_l}{2} - \frac{3v^2}{16c_l^2}\cos\frac{7\theta_l}{2} , \\
f_{22}^b(\theta_l) &= \frac{5}{4}\left(1-\frac{4v^2}{5c_l^2}\right)\cos\frac{3\theta_l}{2} + \frac{3}{4}\left(1-\frac{9v^2}{8c_l^2}\right)\cos\frac{7\theta_l}{2} - \frac{15v^2}{64c_l^2}\cos\frac{11\theta_l}{2} , \\
f_{12}^d(\theta_l) &= -\frac{1}{2}\left(1-\frac{v^2}{2c_l^2}\right)\sin\frac{3\theta_l}{2} + \frac{3v^2}{16c_l^2}\sin\frac{7\theta_l}{2} , \\
f_{12}^b(\theta_l) &= \frac{1}{4}\left(1-\frac{v^2}{2c_l^2}\right)\sin\frac{3\theta_l}{2} + \frac{3}{4}\left(1-\frac{5v^2}{8c_l^2}\right)\sin\frac{7\theta_l}{2} - \frac{15v^2}{64c_l^2}\sin\frac{11\theta_l}{2} .
\end{aligned}$$

From the expression above, we can see that if the crack tip speed $v(t)$ is a constant, i.e. $\dot{v}(t) = 0$, and therefore, $B_l(t) = 0$, equations (5), (6), and (7) give the caustic mapping equation and the initial curve equation corresponding to transient crack growth under constant velocity and varying stress intensity factor. Furthermore, if the time derivative of the dynamic stress intensity factor, $\dot{K}_I^d(t)$ is also zero, $D_l^1\{A_0(t)\}$ will be zero, then we obtain the caustic mapping equation and the initial curve equation for the case of *steady state* crack propagation, in which the asymptotic expansion up to the third term is employed. If in the expression of the first stress invariant, only the singular term remains (pure K_I^d-dominance), then we obtain the equations which are widely used in the classical analysis of the caustic patterns[6,7].

3. INTERPRETATION OF CAUSTIC PATTERNS

For a given specimen with a straight mode-I crack, if the initial/boundary conditions are prescribed, and also if the crack propagation history, i.e. the propagating velocity of the crack tip $v(t)$, is pressumed known, then the history of the dynamic stress intensity factor, $K_I^d(t)$, will be determined, and so will the other quantities in the caustic mapping and the initial curve equations. Therefore, the shape and size of the initial curve and the caustic pattern corresponding to this dynamic crack propagation process for each instant of time can be determined. However in practical applications, we need a means of infering the stress intensity factor history from local near tip measurements since the boundary/initial value problem is usually too difficult to solve. In this section, we will develope a method which can provide the dynamic stress intensity factor and other parameters from the caustic pattern through some experimentally measurable quantities even in presence of highly transient effects.

Since the equations (5), (6), and (7) are too complicated, now we make an assumption that $v/c_l \ll 1$. However, in most cases of practical significance crack tip speeds do not exceed a speed of $0.2c_l$, or approximately $0.5c_R$, where c_R is the material Rayleigh wave speed in plane stress. It is thus felt that assuming that $v/c_l \ll 1$ will lead to a useful and accurate simplification for the mapping equations. Also, we assume that the initial curve can be approximated by a circle, i.e.

$$r_l = \left(\frac{3\alpha_l z_0 chF(v)}{2\sqrt{2\pi}} K_I^d(t)\right)^{\frac{2}{5}} = r_0 \ . \tag{8}$$

Combine these two assumptions, equations (5) and (6) can be rewritten as

$$X_1 = r_0\left\{\cos\theta_l + \frac{2}{3\alpha_l}\left[\cos\frac{3\theta_l}{2} - \frac{\hat{A}(t)r_0}{\hat{K}(t)}\cos\frac{\theta_l}{2} - \frac{\dot{v}(t)r_0}{\alpha_l^4 c_l^2}\left(\cos\frac{\theta_l}{2} - \cos\frac{5\theta_l}{2}\right)\right]\right\} , \tag{9}$$

$$X_2 = r_0\left\{\frac{\sin\theta_l}{\alpha_l} + \frac{2}{3}\left[\sin\frac{3\theta_l}{2} - \frac{\hat{A}(t)r_0}{\hat{K}(t)}\sin\frac{\theta_l}{2} + \frac{\dot{v}(t)r_0}{\alpha_l^4 c_l^2}\left(3\sin\frac{\theta_l}{2} + \sin\frac{5\theta_l}{2}\right)\right]\right\} , \tag{10}$$

where

$$\begin{aligned}
\hat{K}(t) &= z_0 ch\rho(c_l^2 - c_s^2)\frac{3v^2}{4c_l^2}A_0(t) = \frac{z_0 chF(v)}{\sqrt{2\pi}}K_I^d(t) , \\
\hat{A}(t) &= z_0 ch\rho(c_l^2 - c_s^2)\left\{\frac{15v^2}{4c_l^2}A_2(t) + D_l^1\{A_0(t)\}\right\} , \\
F(v) &= \frac{(\alpha_l^2 - \alpha_s^2)(1+\alpha_s^2)}{4\alpha_l\alpha_s - (1+\alpha_s^2)^2} .
\end{aligned}$$

As $\hat{A}(t)r_0/\hat{K}(t) \to 0$ and $\dot{v}(t)/\alpha_l^4 c_l^2 \to 0$, equations (9) and (10) reduce to the parametric equations for caustics obtained on the basis of K_I^d-dominance[6]. Making the above assumptions allows us to relate the two independent unknowns $\hat{K}(t)$ and $\hat{A}(t)$ to two easily measurable dimensions of the caustic curve. The validity of the assumption regarding the circularity of the initial curve will be justified in Section 4 in connection to the Broberg problem.

The two caustic curve dimensions chosen in this analysis are the maximum transverse diameter D of the caustic and the distance between the point of intersection of this diameter with the X_1-axis and the front point of the caustic. This length will be denoted as X, see Fig.2. The above equations can now be used to relate D and X to the instantaneous value of the dynamic stress intensity factor $K_I^d(t)$. Letting $\theta_l = \theta_l^{(D)}$ be the angular coordinate of

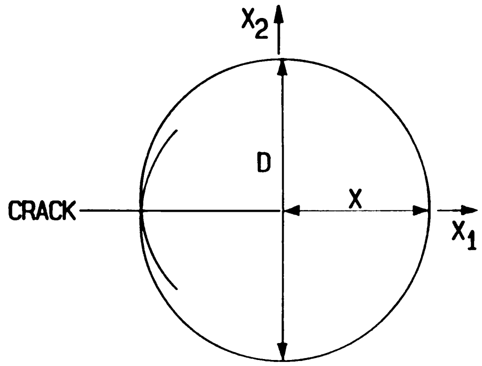

Figure 2: Evaluation of the dynamic stress intensity factor $K_I^d(t)$ by measurement of D and X.

the point $(r_0, \theta_l^{(D)})$ on the initial curve that maps on to the point of the caustic curve where X_2 is maximum, and observing that

$$D = 2X_2(\theta_l^{(D)}) \ , \ \ X = X_1(0) - X_1(\theta_l^{(D)}) \ ,$$

and the maximum condition

$$\frac{\partial X_2}{\partial \theta_l} = 0 \ , \ \ \text{as} \ \ \theta_l = \theta_l^{(D)} \ ,$$

one obtains

$$\frac{D}{r_0} = 2\left(\frac{\sin\theta_l^{(D)}}{\alpha_l} + \frac{2}{3}\sin\frac{3\theta_l^{(D)}}{2}\right) - 2\alpha_l \hat{A}(t) r_0^{-\frac{3}{2}} \sin\frac{\theta_l^{(D)}}{2} + \frac{4\dot{v}(t)r_0}{3\alpha_l^4 c_l^2}\left(3\sin\frac{\theta_l^{(D)}}{2} + \sin\frac{5\theta_l^{(D)}}{2}\right) \ , \tag{11}$$

$$\frac{X}{r_0} = \left(1 + \frac{2}{3\alpha_l} - \cos\theta_l^{(D)} - \frac{2}{3\alpha_l}\cos\frac{3\theta_l^{(D)}}{2}\right) - \hat{A}(t) r_0^{-\frac{3}{2}}\left(1 - \cos\frac{\theta_l^{(D)}}{2}\right) + \frac{2\dot{v}(t)r_0}{3\alpha_l^5 c_l^2}\left(\cos\frac{\theta_l^{(D)}}{2} - \cos\frac{5\theta_l^{(D)}}{2}\right) \ , \tag{12}$$

and

$$\left(\frac{\cos\theta_l^{(D)}}{\alpha_l} + \cos\frac{3\theta_l^{(D)}}{2}\right) - \frac{\alpha_l \hat{A}(t) r_0^{-\frac{3}{2}}}{2}\cos\frac{\theta_l^{(D)}}{2} + \frac{\dot{v}(t)r_0}{3\alpha_l^4 c_l^2}\left(3\cos\frac{\theta_l^{(D)}}{2} + 5\cos\frac{5\theta_l^{(D)}}{2}\right) = 0 \ , \tag{13}$$

where the relation (8) between $\hat{K}(t)$ and r_0 has been used. From the above equations, the three independent unknowns r_0 (or $\hat{K}(t)$), $\theta_l^{(D)}$, and $\hat{A}(t)$ can be obtained by solving above three equations when the two quantities D and X have been measured from the caustic pattern.

Solving for D/r_0 from equations (11) and (13), we get

$$\frac{D}{r_0} = g_1(\theta_l^{(D)})\left\{1 - \frac{2g_1'(\theta_l^{(D)})}{g_1(\theta_l^{(D)})}\tan\frac{\theta_l^{(D)}}{2}\right\}\left\{\frac{1}{2} + \sqrt{\frac{1}{4} + \frac{2\dot{v}(t)D}{\alpha_l^4 c_l^2}\frac{G_2(\theta_l^{(D)})}{[G_1(\theta_l^{(D)})]^2}}\right\} \ , \tag{14}$$

where

$$g_1(\theta_l^{(D)}) = 2\left(\frac{\sin\theta_l^{(D)}}{\alpha_l} + \frac{2}{3}\sin\frac{3\theta_l^{(D)}}{2}\right) \ , \ \ g_2(\theta_l^{(D)}) = \frac{2}{3}\left(3\sin\frac{\theta_l^{(D)}}{2} + \sin\frac{5\theta_l^{(D)}}{2}\right) \ ,$$

and

$$G_1(\theta_l^{(D)}) = g_1(\theta_l^{(D)}) - 2g_1'(\theta_l^{(D)})\tan\frac{\theta_l^{(D)}}{2} \ , \ \ G_2(\theta_l^{(D)}) = g_2(\theta_l^{(D)}) - 2g_2'(\theta_l^{(D)})\tan\frac{\theta_l^{(D)}}{2} \ ,$$

where the prime denotes the derivative with respect to $\theta_l^{(D)}$.

In terms of the dynamic stress intensity factor, by using equation (8), equation (14) can be rewritten as

$$K_I^d(t) = \frac{2\sqrt{2\pi}}{3\alpha_l chz_0 F(v)} \left\{ \frac{D}{g_1(\theta_l^{(D)})} \right\}^{\frac{5}{2}} \left\{ 1 - \frac{2g_1'(\theta_l^{(D)})}{g_1(\theta_l^{(D)})} \tan \frac{\theta_l^{(D)}}{2} \right\}^{-\frac{5}{2}} \left\{ \frac{1}{2} + \sqrt{\frac{1}{4} + \frac{2\dot{v}(t)D}{\alpha_l^4 c_l^2} \frac{G_2(\theta_l^{(D)})}{\left[G_1(\theta_l^{(D)})\right]^2}} \right\}^{-\frac{3}{2}} . \quad (15)$$

Also, from equations (12) and (13), we can get that

$$\frac{X}{r_0} = f_1(\theta_l^{(D)}) \left\{ \frac{1}{2} + \sqrt{\frac{1}{4} + \frac{2\dot{v}(t)X}{\alpha_l^4 c_l^2} \frac{f_2(\theta_l^{(D)})}{\left[f_1(\theta_l^{(D)})\right]^2}} \right\} , \quad (16)$$

where

$$\begin{aligned} f_1(\theta_l^{(D)}) &= 1 + \frac{2}{3\alpha_l} - \left[1 + \frac{2}{\alpha_l^2} \left(\sec \frac{\theta_l^{(D)}}{2} - 1 \right) \right] \cos \theta_l^{(D)} + \frac{2}{\alpha_l} \left(\frac{2}{3} - \sec \frac{\theta_l^{(D)}}{2} \right) \cos \frac{3\theta_l^{(D)}}{2} , \\ f_2(\theta_l^{(D)}) &= \frac{1}{3\alpha_l} \left\{ \left(4 - 3 \sec \frac{\theta_l^{(D)}}{2} \right) \cos \frac{\theta_l^{(D)}}{2} + \left(4 - 5 \sec \frac{\theta_l^{(D)}}{2} \right) \cos \frac{5\theta_l^{(D)}}{2} \right\} . \end{aligned}$$

From equations (14) and (16), one also gets

$$\frac{X}{D} = \frac{f_1(\theta_l^{(D)})}{G_1(\theta_l^{(D)})} \left\{ \frac{1}{2} + \sqrt{\frac{1}{4} + \frac{2\dot{v}(t)X}{\alpha_l^4 c_l^2} \frac{f_2(\theta_l^{(D)})}{\left[f_1(\theta_l^{(D)})\right]^2}} \right\} \left\{ \frac{1}{2} + \sqrt{\frac{1}{4} + \frac{2\dot{v}(t)D}{\alpha_l^4 c_l^2} \frac{G_2(\theta_l^{(D)})}{\left[G_1(\theta_l^{(D)})\right]^2}} \right\}^{-1} . \quad (17)$$

The angle $\theta_l^{(D)}$ that appears in equation (15) is the root of the above trigonometric equation.

Under the fully transient dynamic condition, equations (15) and (17) give the final relation between the dynamic stress intensity factor, $K_I^d(t)$, and the experimentally measurable quantities, D and X. From the equation (15), we can see that for the case of non-uniformly propagating crack, the dynamic stress intensity factor, $K_I^d(t)$, infered from the caustic pattern, does depend on the crack tip acceleration, $\dot{v}(t)$. Another interesting point is that the second braces on the right hand side of the relation (15) is related to the time derivative of the dynamic stress intensity factor and the coefficient of the third term in the asymptotic expansion of the stress field, $A_2(t)$. Actually, the coefficient $A_2(t)$ can be obtained in the following way,

$$\hat{A}(t) = \frac{1}{\alpha_l} \sec \frac{\theta_l^{(D)}}{2} \left\{ g_1'(\theta_l^{(D)}) \left(\frac{r_0}{D} \right)^{\frac{3}{2}} + \frac{2\dot{v}(t)D}{\alpha_l^4 c_l^2} g_2'(\theta_l^{(D)}) \left(\frac{r_0}{D} \right)^{\frac{5}{2}} \right\} D^{\frac{3}{2}} , \quad (18)$$

and

$$A_2(t) = \frac{4c_l^2}{15v^2} \left\{ \frac{\hat{A}(t)}{z_0 ch\rho(c_l^2 - c_s^2)} + \frac{8v^{\frac{1}{2}}(t)}{3\alpha_l^2} \frac{d}{dt} \left[\frac{v^{-\frac{3}{2}}(t)}{\alpha_l} \left(\frac{r_0}{D} \right)^{\frac{5}{2}} D^{\frac{5}{2}} \right] \right\} , \quad (19)$$

where r_0/D is given by equation (14) and $\theta_l^{(D)}$ by equation (17). Once D, X, and $v(t)$ are determined by experiment, $\theta_l^{(D)}$ is first calculated using equation (17) at each instant of time. Then equation (15) is used to obtain $K_I^d(t)$. Subsequently, equations (14), (18), and (19) are used to obtain $\hat{A}(t)$ and $A_2(t)$.

If we only retain the singular term in the asymptotic stress expansion, then in the caustic mapping equations (9) and (10), $\hat{A}(t)r_0/\hat{K}(t)$ and $\dot{v}(t)r_0/\alpha_l^4 c_l^2$ will be zero, and equations (9) and (10) reduce to the same equations used in the classical analysis[6]. Now equation (15) becomes

$$K_I^d(t) = \frac{2\sqrt{2\pi}}{3\alpha_l chz_0 F(v)} \left\{ \frac{D}{g_1(\theta_l^{(D)})} \right\}^{\frac{5}{2}} , \quad (20)$$

and the maximum condition (13) requires that

$$g_1'(\theta_l^{(D)}) = 2\left(\frac{\cos\theta_l^{(D)}}{\alpha_l} + \cos\frac{3\theta_l}{2}\right) = 0 \ , \tag{21}$$

from which the parameter $\theta_l^{(D)}$ can be determined as a function of the crack tip velocity. Define

$$C(v) = \frac{1}{\alpha_l F(v)}\left\{\frac{3.17}{g_1(\theta_l^{(D)})}\right\}^{\frac{5}{2}} \ ,$$

where $C(v)$ is a function of the crack tip velocity, and equation (20) takes the form

$$K_I^d(t) = C(v)\frac{D^{\frac{5}{2}}}{10.7z_0 ch} \ , \tag{22}$$

which has the same form as that given by Rosakis, Duffy, and Freund[8]. Moreover, for the stationary crack, $\alpha_l = 1$, $F(v) = 1$, and equation (21) gives $\theta_l^{(D)} = \theta_0 = 72^o$, and $g(\theta_l^{(D)}) = 3.17$. Then from equation (22), we can get

$$K_I^d(t) = \frac{2\sqrt{2\pi}}{3chz_0}\left(\frac{D}{3.17}\right)^{\frac{5}{2}} \ . \tag{23}$$

This equation holds not only for the stationary crack under dynamic loading, but also for the quasi-static problem, where $K_I^d(t)$ should be replaced by K_I.

4. AN EXAMPLE: BROBERG PROBLEM

In order to illustrate the role of the higher-order terms in the caustic pattern of a non-uniformly propagating crack, and demonstrate that the application of equations (15) and (17) are able to furnish the correct result of the dynamic stress intensity factor, $K_I^d(t)$, the solution of a particular transient boundary value problem concerned with the elastodynamic crack growth is considered. This is the plane strain problem of a crack growing symmetrically from zero initial length at constant velocity under uniform remote tensile stress σ_∞. The plane of deformation is the x_1', x_2'-plane and the crack lies in the interval $-vt < x_1' < vt$, $x_2' = 0$, where v is the constant speed of either crack tip. This is the problem first analyzed by Broberg[9]. It should be noted that although this problem involves constant crack growth velocities, it is highly transient. This is due to the existence of large time derivatives in $K_I^d(t)$ near the instant of initiation.

An expression for the first stress invariant directly ahead of the crack tips is obtained by Freund[10]. On the plane $x_2' = 0$,

$$\sigma_{11} + \sigma_{22} = -2\sigma_\infty\frac{I(v/c_s)}{v}\left(1 - \frac{c_s^2}{c_l^2}\right)\int_{1/c_l}^{t/x_1'}\frac{f(\xi)}{(v^{-1} - \xi)^{\frac{3}{2}}}d\xi \ , \tag{24}$$

where $I(v/c_s)$ is a known function of v, and

$$f(\xi) = \frac{(c_s^{-2} - 2\xi^2)}{(\xi^2 - c_l^{-2})^{\frac{1}{2}}(v^{-1} + \xi)^{\frac{3}{2}}} \ .$$

Focusing on the crack tip moving in the positive x_1'-direction, if the equation (24) is expanded in powers of $x_1 = x_1' - vt$ near $x_1 = 0$, then

$$\sigma_{11} + \sigma_{22} = W(v)\frac{K_I^d(t)}{\sqrt{2\pi}}\left\{x_1^{-\frac{1}{2}} + \frac{1}{vt}\left[\frac{1}{2} + \frac{f'(1/v)}{vf(1/v)}\right]x_1^{\frac{1}{2}}\right\} + o\left(x_1^{\frac{1}{2}}\right) \ , \tag{25}$$

where

$$W(v) = \frac{2(1+\alpha_s^2)(\alpha_l^2 - \alpha_s^2)}{D(v)} \ ,$$

$$K_I^d(t) = \frac{c_s^2 I(v/c_s)D(v)}{\alpha_l v^2}\sigma_\infty\sqrt{\pi vt} \ .$$

If the expansion (25) is compared with the general expansion (4), in which $B_l(t) = 0$ ($\dot{v}(t) = 0$), and $\theta_l = 0, r_l = x_1$, and terms of like powers in distance from the crack tip are equated, then explicit relations for the coefficients in the expansion are obtained as

$$A_0(t) = \frac{2}{3}\frac{W(v)}{\alpha_l^2 - \alpha_s^2}\frac{K_I^d(t)}{\mu\sqrt{2\pi}} = \frac{2\sqrt{2}}{3}\frac{(1+\alpha_s^2)I(v/c_s)}{\alpha_l(1-\alpha_s^2)}\frac{\sigma_\infty}{\mu}\sqrt{vt} \, , \tag{26}$$

$$D_l^1\{A_0(t)\} = \left(1 - \frac{1}{\alpha_l^2}\right)\frac{W(v)}{\alpha_l^2 - \alpha_s^2}\frac{K_I^d(t)}{\mu\sqrt{2\pi vt}} = -\sqrt{2}\frac{(1-\alpha_l^2)(1+\alpha_s^2)I(v/c_s)}{\alpha_l^3(1-\alpha_s^2)}\frac{\sigma_\infty}{\mu}\frac{1}{\sqrt{vt}} \, , \tag{27}$$

$$A_1(t) = 0 \, , \tag{28}$$

$$\begin{aligned} A_2(t) &= \frac{2}{15}\left[\frac{5}{4} + \frac{5}{4\alpha_l^2} + \frac{f'(1/v)}{vf(1/v)}\right]\frac{W(v)}{\alpha_l^2 - \alpha_s^2}\frac{K_I^d(t)}{\mu\sqrt{2\pi vt}} \\ &= \frac{2\sqrt{2}}{15}\left[\frac{5}{4} + \frac{5}{4\alpha_l^2} + \frac{f'(1/v)}{vf(1/v)}\right]\frac{(1+\alpha_s^2)I(v/c_s)}{\alpha_l(1-\alpha_s^2)}\frac{\sigma_\infty}{\mu}\frac{1}{\sqrt{vt}} \, . \end{aligned} \tag{29}$$

Since the coefficients of $D_l^1\{A_0(t)\}$ and $A_2(t)$ are proportional to $1/\sqrt{t}$, the third term in the near tip asymptotic expansion of the first stress invariant can be very large during the early stages of crack growth, possibly dominating the square root singular term under certain conditions, and therefore in this example, even though the crack tip speed is constant, the transient effects do exist in the near tip field.

For this particular problem, normalize the caustic mapping equations (5) and (6), and the initial curve equation (7) with the length r_0, which is the radius of the approximated circular initial curve and is related to the value of the dynamic stress intensity factor, $K_I^d(t)$, of Broberg problem by equation (8). Because of the length limitation, only the normalized caustic mapping equations are presented

$$\begin{aligned} \frac{X_1}{r_0} = &\left(\frac{r_l}{r_0}\right)\cos\theta_l + \frac{2}{3\alpha_l}\left(\frac{r_l}{r_0}\right)^{-\frac{3}{2}}\cos\frac{3\theta_l}{2} \\ &- \frac{2}{3\alpha_l}\left(\frac{r_0}{vt}\right)\left\{\left[\frac{5}{4} + \frac{5}{4\alpha_l^2} + \frac{f'(1/v)}{vf(1/v)}\right]\cos\frac{\theta_l}{2} - 2\left[\left(1 - \frac{v^2}{4c_l^2}\right)\cos\frac{\theta_l}{2} - \frac{v^2}{8c_l^2}\cos\frac{5\theta_l}{2}\right]\right\}\left(\frac{r_l}{r_0}\right)^{-\frac{1}{2}} \, , \end{aligned} \tag{30}$$

$$\begin{aligned} \frac{X_2}{r_0} = &\left(\frac{r_l}{r_0}\right)\frac{\sin\theta_l}{\alpha_l} + \frac{2}{3}\left(\frac{r_l}{r_0}\right)^{-\frac{3}{2}}\sin\frac{3\theta_l}{2} \\ &- \frac{2}{3}\left(\frac{r_0}{vt}\right)\left\{\left[\frac{5}{4} + \frac{5}{4\alpha_l^2} + \frac{f'(1/v)}{vf(1/v)}\right]\sin\frac{\theta_l}{2} - 2\left[\left(1 - \frac{3v^2}{4c_l^2}\right)\sin\frac{\theta_l}{2} - \frac{v^2}{8c_l^2}\sin\frac{5\theta_l}{2}\right]\right\}\left(\frac{r_l}{r_0}\right)^{-\frac{1}{2}} \, . \end{aligned} \tag{31}$$

We can see that the cosfficients of higher-order terms in the nondimensional caustic mapping equations, are proportional to a nondimensional parameter r_0/vt, and this property can be found in the normalized initial curve equation too. As $r_0/vt \to 0$, the expressions of the caustic mapping equations and the initial curve equation will coincide with the expressions which correspond to K_I^d-dominance. As we have shown the time derivative of the dynamic stress intensity factor is proportional to $1/\sqrt{t}$, so as $t \to \infty$, $r_0/vt \to 0$ which means that $\dot{K}_I^d(t) \to 0$, and K_I^d-dominance is achieved at long times after initiation. On the other hand, $r_0/vt \to 0$ can also be achieved by $r_0 \to 0$ for any $t > 0$, or the size of the initial curve is very *small*. In this small region, the stress state is apparently K_I^d-dominant. For a fixed r_0, $r_0/vt \to \infty$ at short times after initiation ($\dot{K}_I^d(t) \to \infty$) and therefore transient effects are important. So the change of the nondimensional parameter r_0/vt from zero to infinity characterizes the relative influence of transients on caustic shape and size.

A qualitative discussion of the influence of higher-order terms and crack tip velocity on the caustic and initial curve shapes is presented in Fig.3 and Fig.4. Fig.3 shows the influence of crack tip velocity on the caustic mapping for $r_0/vt = 0.3$. It is obvious that in the range $0.1 \leq v/c_s \leq 0.5$, changes in crack tip velocity do not markedly influence the caustic shape. The initial curve also remains almost circular. The results displayed in Fig.4 are more striking. Here, the crack tip velocity is fixed ($v/c_s = 0.3$). The ratio r_0/vt is varied to investigate the effect of transients. Indeed, variation of r_0/vt from 0 to 0.5 creates rather large variations in caustic shape. The value of

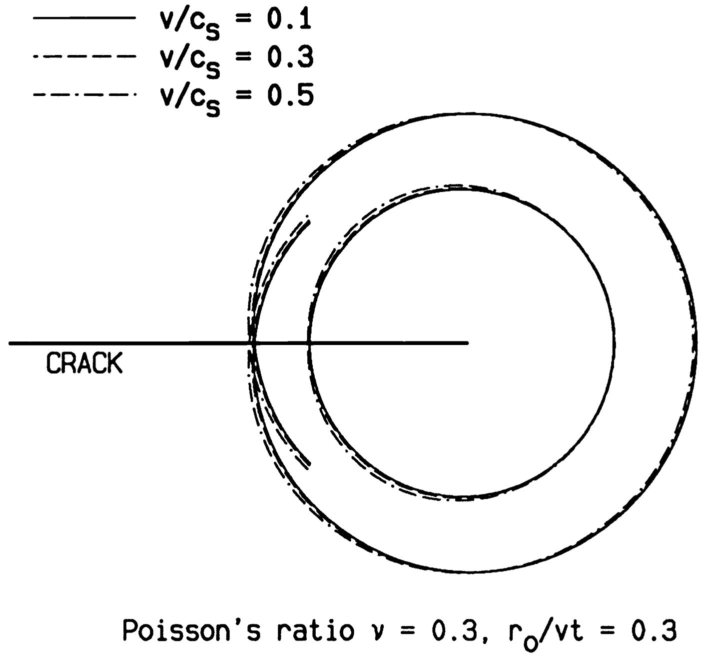

Figure 3: Three-term simulations of the initial and caustic curves corresponding to Broberg problem for different propagation velocity of the crack tip, and for $r_0/vt = 0.3$.

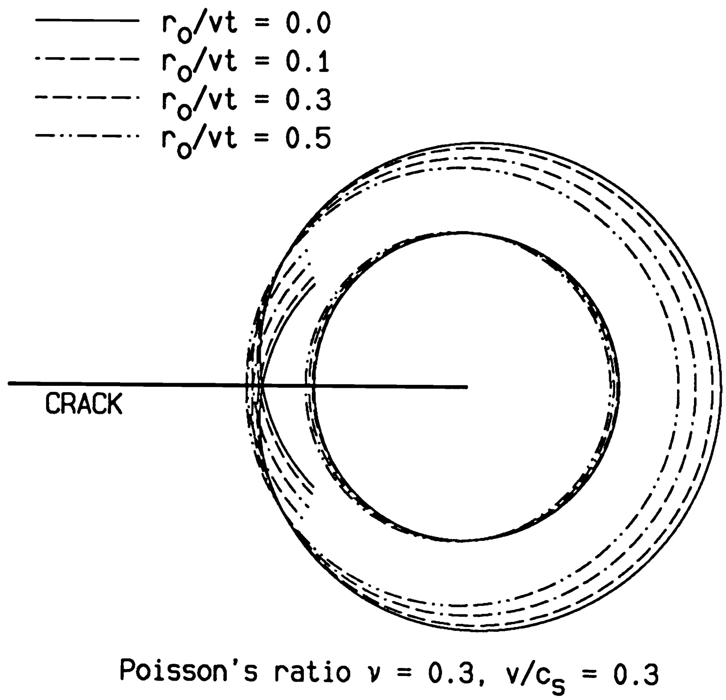

Figure 4: Three-term simulations of the initial and caustic curves corresponding to Broberg problem for different value of r_0/vt, which represents the scale of the transient effects, and for $v/c_s = 0.3$.

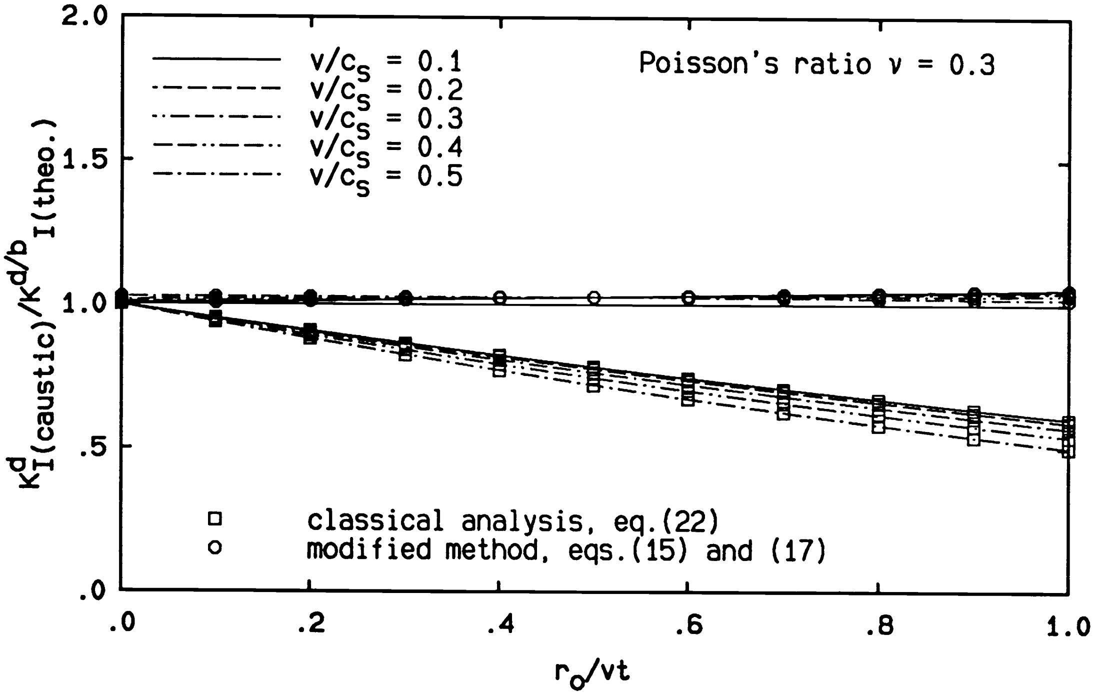

Figure 5: Comparison of dynamic stress intensity factor inferred from the modified method and classical analysis for different value of r_0/vt and different crack propagation velocity.

$r_0/vt = 0$ corresponds to caustic shape obtained by the classical (K_I^d-dominant) analysis of caustics. The differences in D and X observed for other values of r_0/vt are an indication of the error in K_I^d measurement if the classical analysis of caustics is used. On the other hind, it is very interesting to note that the initial curve is hardly influenced by the value of r_0/vt. It remains almost perfectly circular with a radius $r_l = r_0$ as assumed by equation (8) of our analysis. We feel that this provides a strong justification for our simplifying assumption.

Quantitative estimates of the error incurred by the classical interpretation of caustics during crack growth are presented in Fig.5. Here the ratio $K_I^d(t)_{(caustic)}/K_I^d(t)_{(theo.)}$ is presented as a function of the parameter r_0/vt for different crack tip velocities. As anticipated earlier as $r_0/vt \to 0$, the classical analysis becomes accurate (either zero initial curve or long times after initiation). However as $r_0/vt \to \infty$, we observe large deviations of $K_I^d(t)_{(caustic)}$ relative to $K_I^d(t)_{(theo.)}$, which is known prior (see lines with square symbols). The figure also presents the same ratio obtained if the numerically constructed caustics are analyzed on the basis of our improved method (equation (15)). As it is obvious from the lines marked by the circles, errors of less than 5% are obtained. In both cases it is shown that the effect of velocity is small especially when the improved analysis is used.

5. CONCLUSIONS

Motivated by recent experimental evidences[3,4] that show the inadequacy of the classical analysis of caustics in furnishing accurate values of K_I^d in the presence of transient effects, a modified analysis of the technique is presented. The analysis is based on a fully transient higher-order expansion recently developed by Freund and Rosakis[1]. The improved analysis of caustic patterns includes the influence of transients resulting because of the existence of non-uniform $K_I^d(t)$ and $v(t)$ histories (effects of $\dot{K}_I^d(t)$ and $\dot{v}(t)$). The analysis can be used to obtain $K_I^d(t)$ as well as the values of higher-order terms in terms of the geometrical characteristics of the caustic curves. The resulting expressions contain the classical results (K_I^d-dominant analysis) as special cases. The relative performance of the improved and the classical analyses is compared. This is done by considering the Broberg problem as a model of transient crack growth, generating numerical caustics and analyzing them on the basis of either analysis. The inadequacy of the classical method of obtaining K_I^d from caustics is thus demonstrated.

6. REFERENCES

1. L. B. Freund and A. J. Rosakis, "The Structure of the Near Tip Field during Transient Elastodynamic Crack Growth," (submitted to *Journal of the Mechanics and Physics of Solids*), 1991.

2. K. Takahashi and K. Arakawa, "Dependence of Crack Acceleration on the Dynamic Stress-Intensity Factor in Polymers," *Experimental Mechanics*, vol.27, no.2, pp.195-199, 1987.

3. S. Krishnaswamy and A. J. Rosakis, "On the Extent of Dominance of Asymptotic Elastodynamic Crack-Tip Fields: Part I - An Experimental Study Using Bifocal Caustics," *Journal of Applied Mechanics*, vol.58, no.1, pp.87-94, 1991.

4. S. Krishnaswamy, H. V. Tippur, and A. J. Rosakis, "Measurement of Transient Crack Tip Deformation Fields Using the Method of Coherent Gradient Sensing," Caltech Report SM 90-1 (submitted to *Journal of the Mechanics and Physics of Solids*), 1990.

5. A. J. Rosakis and A. T. Zehnder, "On the Method of Caustics: An Exact Analysis Based on Geometrical Optics," *Journal of Elasticity*, vol.15, no.4, pp.347-368, 1985.

6. A. J. Rosakis, "Analysis of the Optical Method of Caustics for Dynamic Crack Propagation," *Engineering Fracture Mechanics*, vol.13, pp.331-347, 1980.

7. J. Beinert and J. F. Kalthoff, "Experimental Determination of Dynamic Stress-Intensity Factors by Shadow Patterns," in *Mechanics of Fracture*, vol.VII, edited by G. Sih, Sijthoff and Noordhoff, pp.281-330, 1981.

8. A. J. Rosakis, J. Duffy, and L. B. Freund, "The Determination of Dynamic Fracture Toughness Of AISI 4340 Steel by the Shadow Spot Method," *Journal of the Mechanics and Physics of Solids*, vol.32, pp.443-460, 1984.

9. K. B. Broberg, "The Propagation of a Brittle Crack," *Archiv fur Fysik*, vol.18, pp.159-192, 1960.

10. L. B. Freund, *Dynamic Fracture Mechanics*, Cambridge University Press, 1990.